JOURNAL OF GEOPHYSICAL RESEARCH, VOL. 99, NO. E5, PAGES 10,867–10,879, MAY 25, 1994

Estimation of grain sizes and mixing ratios of fine powder mixtures of common geologic minerals

Takahiro Hiroi

Solar System Exploration Division, NASA Johnson Space Center, Houston, Texas

Carlé M. Pieters

Department of Geological Sciences, Brown University, Providence, Rhode Island

Abstract. Two different approaches for modeling reflectance spectra of intimate mixtures, Hapke's model and the isograin model, are used to estimate grain sizes and mixing ratios of powder mixtures of three geologic minerals: olivine, orthopyroxene, and plagioclase. In Hapke's model, scattering and extinction efficiencies are mixed separately, and both models employ semiempirical refractive index spectra for component minerals. Mixing ratios of mixtures of grain size 45-75 μm are well estimated by both models assuming a common grain size of 60 μm and optimizing the constants for the single-particle scattering. For each model, effective grain size ratios for mineral constituents in mixtures of grain size <25 μm, are derived successfully that allows mineral abundances to be accurately predicted within ~4 wt%. On the other hand, neither model can accurately predict mineral reflectance spectra for its smaller grain sizes (<25 and 25-45 μm) using an absorption coefficient spectrum derived from a larger grain size (45-75 μm). The errors in both models are significantly reduced if surface roughness effects of the smaller grain-size fractions are modeled.

1. Introduction and Summary

Theoretical approaches to the nature of reflectance spectra of mineral mixtures are very important for better utilization of data obtained by remote sensing [*Clark and Roush*, 1984]. The estimation of grain sizes and mixing ratios of mineral mixtures derived from their reflectance spectra, however, has exhibited two kinds of problems. One is a small but systematic deviation of the calculated mixing ratios from the actual ones [*Mustard and Pieters*, 1989; *Johnson et al.*, 1992]. The other is unusual behavior of reflectance spectra of the smallest grain-size fractions such as <25 μm [*Crown and Pieters*, 1987; *Johnson et al.*, 1992].

Some of the systematic deviations of calculated mixing ratios from the actual ones, may be due to the different grain shapes and size distributions of component minerals. *Hiroi and Pieters* [1992] demonstrated that the difference of grain shapes of component minerals can change their effective grain sizes and apparent mixing ratios. As described in subsequent sections, introducing the appropriate effective grain size for each component mineral may reduce the problem. The unusual behavior sometimes observed for reflectance spectra of the smallest grain size fractions (shallower absorption bands and lower reflectance than theoretically expected) may be due to a combination of very small effective grain sizes and the small-scale surface roughnesses of powder samples. Both the effective grain size and the surface roughness can be incorporated with virtually any reflectance models such as Hapke's model of bidirectional reflectance [*Hapke*, 1981] and the isograin model [*Hiroi and Takeda*, 1990; *Hiroi and Pieters*, 1992].

Paper number 94JE00841.
0148-0227/94/94JE-00841$05.00

In this paper, reflectance spectra of three grain size fractions (<25, 25-45, and 45-75 μm) of common geologic minerals (olivine, pyroxene, and plagioclase) and their mixtures are studied by Hapke's model and the isograin model. Instead of the normal method of mixing single scattering albedos in Hapke's model, its scattering and extinction efficiencies are mixed separately by employing semiempirical refractive index spectra for component minerals. Mixing ratios of mixtures of grain size 45-75 μm are well estimated by both models assuming a common grain size of 60 μm and optimizing the constants for the phase function (Hapke) and the directional scattering fractions (isograin). Mixing of fine-grain minerals is much more sensitive to their effective grain size estimates. For each model, effective grain size ratios for mineral constituents in the <25 μm mixtures are derived and successfully used. Optimization of effective grain size allows mineral abundances to be accurately predicted within ~4 wt%.

On the other hand, neither model can accurately predict mineral reflectance spectra for smaller size fractions (<25 and 25-45 μm) using an absorption coefficient spectrum derived from a larger grain size (45-75 μm). If surface roughness effects of the smaller grain-size fractions are considered, the errors in both models are significantly reduced. A formulation that approximates surface roughness is described that can be used successfully with either model.

2. Experimental Procedures

Large green olivine crystals and a plagioclase rock (Split Rock, Minnesota) were purchased from WARD'S Natural Science Establishment, Inc., and a pyroxene-rich sand (Chichijima, Bonin Islands, Japan) was supplied from the University Museum of the University of Tokyo, Japan. Orthopyroxene crystals were hand-picked from the pyroxene sand. Each of these

samples was ground and sieved into three grain-size fractions: <25, 25-45, and 45-75 μm. The <25μm fraction was dry sieved and the others were wet sieved with water. Sixteen mixtures were prepared from 45-75μm fractions of three minerals, and seven mixtures from <25μm fractions. One of the olivine crystals was polished using 0.03-μm polishing power producing a flat surface of 1.128 mm in thickness and about 1 cm in diameter.

Bidirectional diffuse reflectance spectra (0.3-2.6 μm) of the above powders were measured at 30° incidence and 0° emergence angles. Specular reflectance and transmittance spectra of the olivine single crystal were measured at 13° and 0° incidence angles, respectively. A pressed halon and an aluminum mirror were used as standards for diffuse and specular reflectance measurements, respectively. Measured raw reflectances were corrected based on data by the National Bureau of Standards. All the spectra were measured at RELAB in Brown University. The details of RELAB are described in *Pieters* [1983] and in the RELAB Users Manual.

Chemical compositions of the olivine and pyroxene powders varied slightly from grain to grain and were estimated from electron microprobe measurements. Detailed chemical composition of plagioclase was measured by *Mustard and Pieters* [1989]. Specific gravities of those three minerals were carefully measured by water displacement, and their refractive indices were measured by oils.

3. Experimental Results

Shown in Figure 1 are reflectance spectra of three grain size fractions <25, 25-45, and 45-75 μm of olivine, pyroxene, and plagioclase obtained at 30° incidence and 0° emergence angles. These three geologic minerals have very different absorption features from one another. Most of the prominent features are due to ferrous iron in different crystallographic sites. Although smaller grain size fractions usually have higher reflectances and shallower absorption bands, reflectances of <25 μm fractions are lower than expected. For example, the <25 μm fraction of olivine has a lower reflectances than the 25-45 μm fraction at wavelengths longer than 1.7 μm in Figure 1.

Reflectance spectra of seven tricomponent mixtures of fractions <25 and 45-75 μm, are shown in Figure 2. Mixing ratios of component minerals will be listed later in a table together with the calculated values by reflectance models. These reflectance spectra appear to have systematic differences between fractions of 45-75 and <25 μm, which suggests that it may be possible to estimate their grain sizes and mixing ratios simultaneously.

Shown in Figure 3 are specular reflectance (13° incidence) and transmittance (0° incidence) of a single crystal of olivine. They were converted into refractive index and absorption coefficient by Fresnel theory. The imaginary part of the refractive index of this olivine is about 1/100 of the real part and can be neglected in most calculations of surface reflectivities. The imaginary part of refractive index can also be neglected for pyroxene and plagioclase in this study because their absorption bands are also weak. Refractive indices, specific gravities, and the range of chemical compositions of three minerals, are listed in Table 1.

For simplicity and reduction of noise in calculations, refractive index spectra were modeled as linear functions of wavenumber

$$n(\lambda) = c_0 + c_1 / \lambda \quad (1)$$

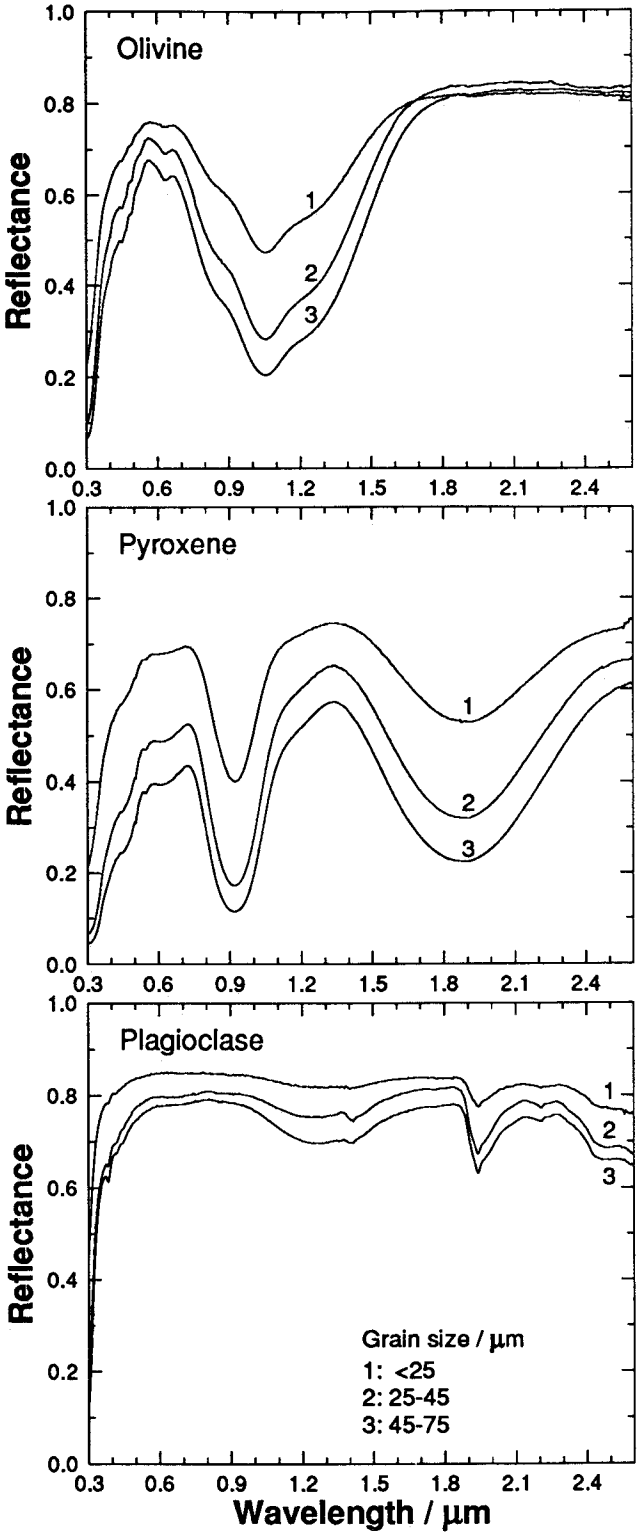

Figure 1. Bidirectional reflectance spectra (30° incidence, 0° emergence) of common geologic mineral powders: olivine, pyroxene, and plagioclase of grain sizes <25, 25-45, and 45-75 μm.

where $n(\lambda)$ indicates refractive index at wavelength λ, and c_0 and c_1 are constants. Shown in Figure 4a is such a function for the olivine crystal calculated by the least squares method. Because olivine crystals used in our study had a range of chemical composition (Fa 11-15 in Table 1), refractive index of

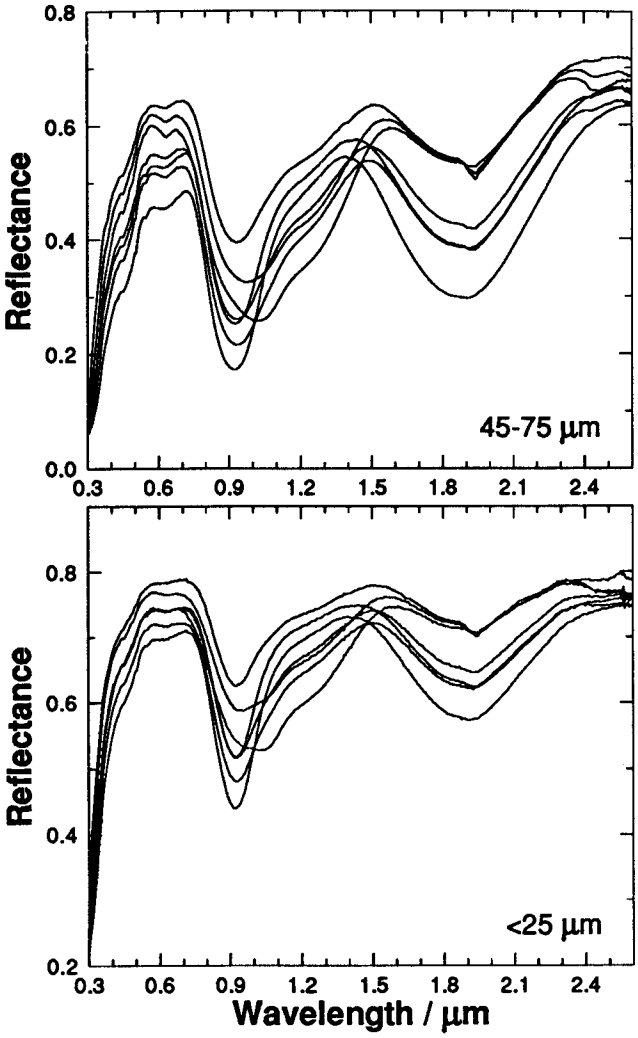

Figure 2. Reflectance spectra of tricomponent mixtures of olivine, pyroxene, and plagioclase of grain sizes 45-75 and <25 μm. The abundance of each mineral in these seven mixtures is itemized in Tables 2 and 3.

this particular crystal may differ somewhat from the one measured by oils using many olivine grains taken from the powder sample. Therefore, c_0 and c_1 values in equation (1) were scaled keeping the c_0-1 : c_1 ratio constant, so that $n(0.55\ \mu m)$ can match with the value measured by oils while keeping $n(\lambda) > 1$ at every wavelength λ. Shown in Figure 4b are such semiempirical refractive index spectra for the three mineral samples in this study. Calculated c_0 and c_1 values are listed in Table 1.

4. Reflectance Models

Aspects of the two models used in this analysis are described below. Both models are intended to be used with intimate mixtures of minerals and describe "nonlinear" mixing of materials. Although they each have different assumptions and approximations in modeling how light interacts with materials, generally comparable forms of the two models have been used here.

As described by *Hapke* [1981], bidirectional reflectance R of powder relative to Lambertian surface with no preferential escape of singly scattered light, is expressed by

$$R(\theta_i,\theta_e,w) = \frac{w}{4}\frac{1}{\mu_i+\mu_e}\left[P(g,w) + H(\mu_i,w)H(\mu_e,w) - 1\right] \quad (2a)$$

$$\mu_i = \cos\theta_i, \quad \mu_e = \cos\theta_e, \quad g = |\theta_e - \theta_i| \quad (2b)$$

where θ_i, θ_e, and g are incidence, emergence, and phase angles, respectively, w is called the single scattering albedo which is a function of wavelength, $P(g,w)$ is the average particle phase function, and $H(\mu,w)$ is the solution of the integral equation

$$H(\mu,w) = 1 + \frac{1}{2}w\mu H(\mu,w)\int_0^1 \frac{H(\mu',w)}{\mu+\mu'}d\mu' \quad (3)$$

which was numerically solved by *Chandrasekhar* [1960] for a limited number of (μ,w) values. *Hapke* [1981] presented a practical approximation for the H function:

$$H_{\text{Hapke}}(\mu,w) = \frac{1+2\mu}{1+2\mu\sqrt{1-w}} \quad (4)$$

A more accurate approximation can be obtained by using Chandrasekhar's exact solution data to constrain Hapke's approximation:

$$H(\mu,w) = c(\mu,w)H_{\text{Hapke}}(\mu,w) \quad (5)$$

where $c(\mu,w)$ is a coefficient to adjust Hapke's H function $H_{\text{Hapke}}(\mu,w)$ to Chandrasekhar's exact solution. The $c(\mu,w)$ val-

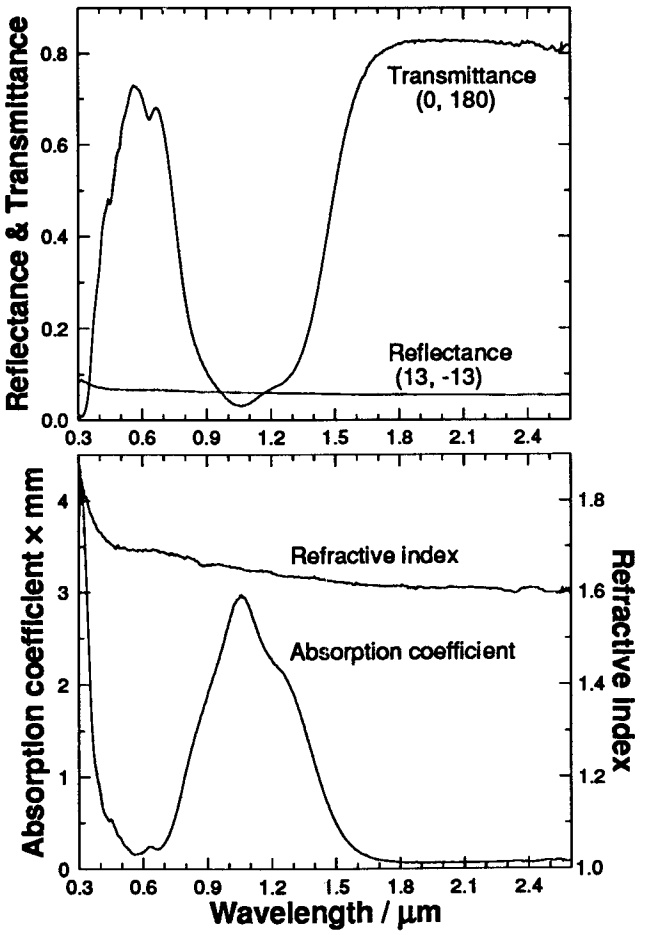

Figure 3. Specular reflectance and transmittance spectra of a polished olivine single crystal of 1.128 mm in thickness, and refractive index and absorption coefficient spectra of the olivine derived by Fresnel theory.

Table 1. Measured Chemical Compositions, Specific Gravities, Refractive Indices, and Assumed Refractive Index Spectra $n(\lambda)$ of Three Component Minerals, Where λ Indicates Wavelength

	Chemical Composition	Specific Gravity	Refractive Index	$n(\lambda) = c_0 + c_1 / \lambda$ c_0	c_1 / μm
Olivine	Fa 11-15	3.461	1.670	1.5493	0.066398
Pyroxene	Fs 10-15	3.425	1.670	1.5493	0.066398
Plagioclase	An 78.4 Ab 21.2*	2.729	1.568	1.4657	0.056290

* *Mustard and Pieters* [1989].

ues are calculated by cubic spline interpolation for the (μ, w) values that are not included in *Chandrasekhar* [1960]. Examples of $c(\mu, w)$ and the modified Hapke's H function in equation (5) are shown in Figure 5.

The average particle phase function $P(g, w)$ in equation (2a) is assumed to be a linear function of the single scattering albedo w:

$$P(g,w) = p_0(g)[1 + p_1(g)w], \quad p_0(g) > 0, \quad p_1(g) > -1 \tag{6}$$

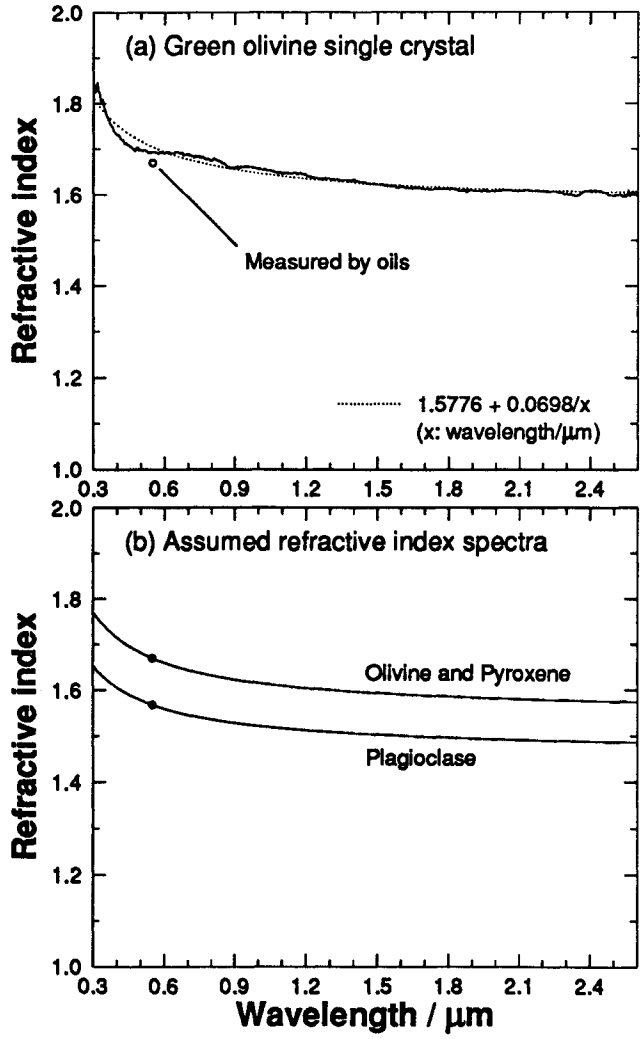

Figure 4. (a) A least squares fit of refractive index spectrum of olivine by a linear function of wavenumber, and refractive index measured by oils. (b) Scaled refractive index functions for olivine, pyroxene, and plagioclase used in this study. Open circles are refractive indices measured by oils.

In the analysis described in subsequent sections, equation (2a) is normalized by its value for $P(g, w)=1$ and $w=1$ in order to better compare the calculations with the actual measurements:

$$R_{\text{obs}}(\theta_i, \theta_e, w) = R(\theta_i, \theta_e, w) / R(\theta_i, \theta_e, w = 1, P = 1) \tag{7}$$

The above form of Hapke's model is used in this study for the purpose of estimations of grain sizes and mixing ratios.

The single scattering albedo w is defined by

$$w = < Q_S > / < Q_E > \tag{8}$$

where Q_S and Q_E indicate scattering and extinction efficiencies of component mineral grains, and angle brackets indicate the average value of the quantity inside it. Q_S and Q_E should be mixed in

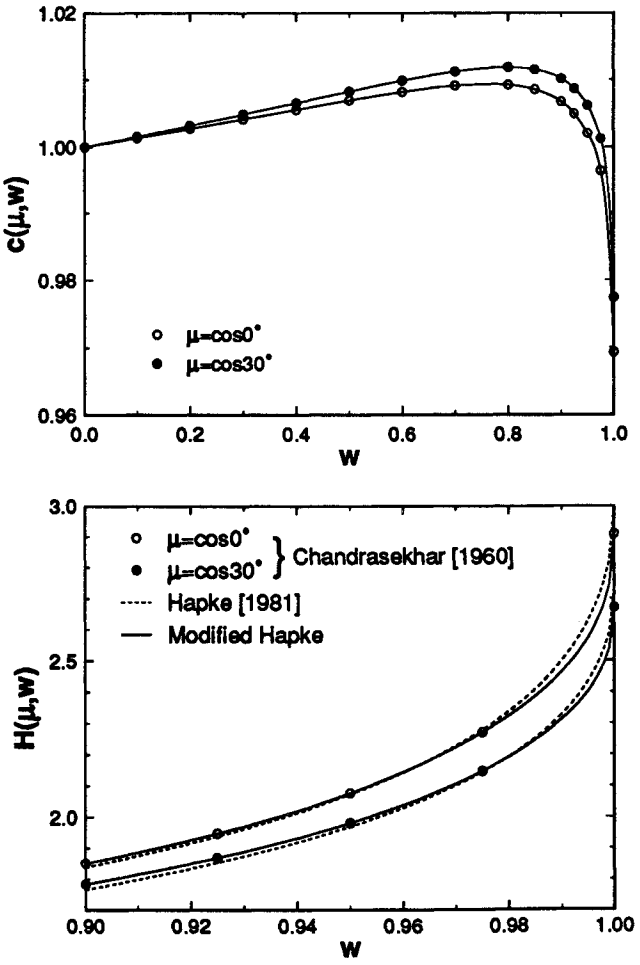

Figure 5. Examples of the correction coefficient $c(\mu, w)$ and the modified Hapke's H function for incidence or emergence angles of 0° and 30°.

proportion to the scattering cross sections of component minerals, namely,

$$< Q_S >= \sum_i \sigma_i Q_{Si}, \quad < Q_E >= \sum_i \sigma_i Q_{Ei} \tag{9a}$$

$$\sigma_i \propto M_i / \rho_i d_{ei} \tag{9b}$$

where Q_{Si} and Q_{Ei} are scattering and extinction efficiencies of component i, respectively, and the linear combination coefficient σ_i is proportional to the total geometric cross section of component i derived from its mass fraction M_i, density ρ_i, and effective grain size d_{ei}.

The concept of the effective grain size is described by *Hiroi and Pieters* [1992] as a common measure of both the average light path length inside each grain and the scattering cross-sectional area of the same grain. Only when Q_E values are common for all the components can the single scattering albedo w in equation (8) be transformed to a linear combination of the single scattering albedo w_i of each component i:

$$w = \sum_i \sigma_i w_i, \quad w_i = Q_{Si} / < Q_E > \tag{10}$$

In order to obtain two quantities Q_S and Q_E of each component mineral from a single reflectance measurement at each wavelength, Q_S and Q_E must be expressed by absorption coefficient and refractive index of the mineral, using the semiempirical refractive index spectra in Figure 4b. Isotropic scattering of light by a mineral grain is illustrated in Figure 6a. Part of the incident light onto a grain is transmitted without being reflected (Q_T), part is scattered to other directions (Q_S), and the rest is absorbed. Because Q_E is the fraction of light that is lost after going through a grain by its definition, Q_E is calculated from the transmitting efficiency Q_T:

$$Q_E = 1 - Q_T \tag{11}$$

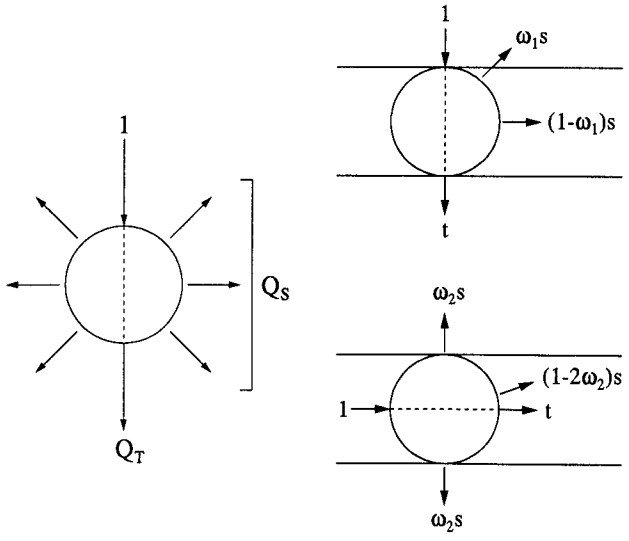

(a) Hapke's model (b) Isograin model

Figure 6. (a) The scattering efficiency Q_S and transmitting efficiency Q_T of a mineral grain in Hapke's isotropic model. (b) The scattering activity s and transmitting activity t of a mineral grain and constants ω_1 and ω_2 in the isograin model.

Q_S and Q_T are assumed to be expressed by a simple multireflection formula

$$Q_S = r_E + (1 - r_E)(1 - r_I) r_I p / (1 - r_I p) \tag{12a}$$

$$Q_T = (1 - r_E)(1 - r_I) p \tag{12b}$$

$$p = \exp(-\alpha d_e) \tag{12c}$$

where r_E and r_I are the surface reflectivities from outside and inside the grain, respectively, α is absorption coefficient of the mineral crystal, d_e is the effective grain size, and p is an absorption variable (not to be confused with p_0 and p_1 in equation (6) for the phase function). The values of r_E and r_I are identical to S_E and S_I of *Hapke* [1981], respectively, and they are calculated from refractive index of the mineral for the isotropic incident light by Fresnel theory (Figure 6 of *Hapke* [1981] or Figure 5 of *Hiroi and Pieters* [1992]). The expression for Q_S in equation (12a) is different from equation (24) of *Hapke* [1981] that assumes the internal scattering of each grain and treats Q_E as a separate constant. Equations (12b) and (12a) treat the single transmission and scattering separately so that they can take care of a part of the anisotropy caused by the change of opacity of each grain.

The second nonlinear mixing model used in this analysis is the isograin model described by *Hiroi and Pieters* [1992]. Shown in Figure 6b is the relation between scattering and transmitting activities of the isograin model. The isograin model has a multilayer structure in which only three integrated light streams are considered: upper, lower, and horizontal. Each grain in each layer has its scattering activity s and transmitting activity t, which are the functions of wavelength. Two constants ω_1 and ω_2 express scattered light fractions to upper, lower, and horizontal directions. Derivation of these constants for various materials are described in detail by *Hiroi and Pieters* [1992]. In this model, total reflectance R_∞ of the infinite number of layers is expressed by

$$R_\infty = R / (B + \sqrt{B^2 - R^2}), \quad B = (1 + R^2 - T^2) / 2 \tag{13a}$$

$$R = \omega_1 s + \omega_2 s x, \quad T = t + \omega_2 s x \tag{13b}$$

$$x = (1 - \omega_1) s / [1 - t - (1 - 2\omega_2) s] \tag{13c}$$

For mineral mixtures, s and t should be mixed in the same way as in equation (9):

$$s = \sum_i \sigma_i s_i, \quad t = \sum_i \sigma_i t_i \tag{14}$$

where s_i and t_i are the scattering and transmitting activities of component i, respectively. The scattering and transmitting activities of a single mineral grain are assumed to be expressed by

$$s = r_E + (1 - r_E)(1 - r_I) r_I p / (1 - r_I^2 p^2) \tag{15a}$$

$$t = (1 - r_E)(1 - r_I) p / (1 - r_I^2 p^2) \tag{15b}$$

$$p = \exp(-\alpha d_e) \tag{15c}$$

where every term has the same meaning as in equation (12).

5. Surface Roughness Formulation

The effect of surface roughness on the grain-size scale is formulated in this section. Each powder sample in this study was put into a dish, and its surface was cut with a spatula to make a smooth surface for the reflectance measurement. However, none of the samples is free of surface roughness in microscopic scales. Surface roughness is expected to be more important for the samples of higher reflectances and greater shadowing effect.

Shown in Figure 7 is a simple formulation of the surface-roughness effect. There are assumed to be surface holes of depth $n_h d_e$ at every distance of $m_h d_e$, where d_e indicates the effective grain size of the powder sample. One part of unit incident light (I_i) shines onto the side of the hole and does not directly contribute to the reflected light but tends to compensate the loss of the internally scattered light from the opposite side of the hole. The same amount of incident light (I_i) is transmitted through the edge of the hole before being reflected by the bottom surface, and another part of the incident light (I_e) is reflected from the bottom surface of the hole and is also transmitted through the edge. Two transmitted components contribute to the reflected light as $I_i T_i$ and $I_e T_e$, where T_i and T_e indicate transmittances of the hole edges. Those I and T values are the functions of the incidence angle (θ_i), the emergence angle (θ_e), and the single-grain transmission (t):

$$I_i = I_h(\theta_i), \quad I_e = I_h(\theta_e), \quad T_i = T_h(\theta_i), \quad T_e = T_h(\theta_e) \tag{16a}$$

$$I_h(\theta) = (n_h / m_h)\tan\theta \tag{16b}$$

$$T_h(\theta) = (1/n_h)t^{1/\cos\theta}(1 - t^{n_h/\cos\theta}) / (1 - t^{1/\cos\theta}) \tag{16c}$$

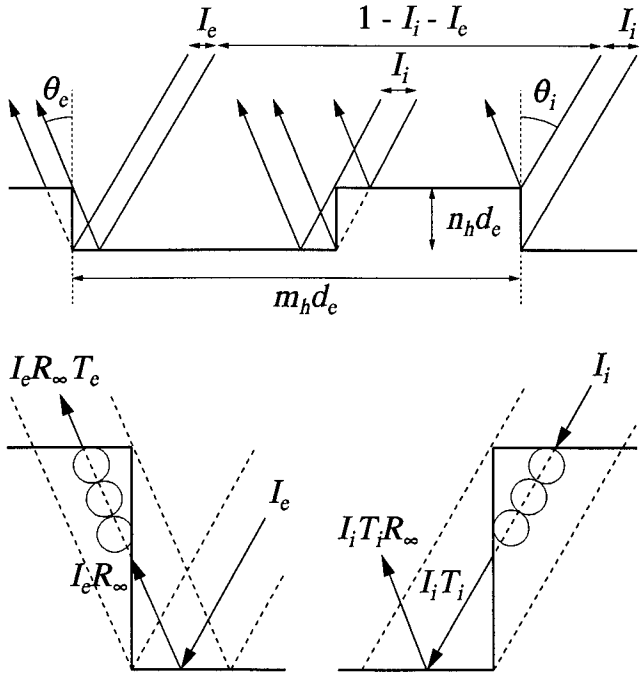

Figure 7. A sketch showing idealized grain features used to formulate surface roughness.

Actual reflectance of the sample with a surface roughness described above becomes

$$R_\infty(m_h, n_h) = (1 - I_i - I_e + I_i T_i + I_e T_e) R_\infty(n_h = 0) \tag{17}$$

where $R_\infty(n_h = 0)$ indicates reflectance with no surface roughness. The scheme in Figure 7 is valid only when

$$m_h \geq 2n_h \tan\theta_m, \quad \theta_m = \max(|\theta_i|, |\theta_e|) \tag{18}$$

The incident light (I_i) onto the sidewall of the hole tends to compensate the loss of light from the other sidewall of the hole. Therefore, those effects are neglected in this formulation.

Equations (16) and (17) are expressed in notations of the isograin model. A similar formula for Hapke's model involves replacing t and R_∞ with Q_T and R_{obs}, respectively.

6. Results of Calculations

Reflectance Models With Mixtures of Grain Size 45-75 μm

Reflectance spectra of 16 mixtures of olivine, pyroxene, and plagioclase of grain size 45-75 μm, were used for testing the validity of the isograin model and Hapke's model because the grain sizes of those mixtures seemed to be well defined. All the end-member minerals were assumed to have the common effective grain size d_e=60 μm, a possible average grain size. Only the relative values of the effective grain sizes are important in this study, although the actual effective gain size should be smaller than the average grain size for any grain shapes [*Hiroi and Pieters*, 1992].

Absorption coefficient spectra of three component minerals (45-75 μm) were derived from their measured reflectance spectra in Figure 1 by equations (2), (4), (5), (6), (7), (8), (11), and (12) for Hapke's model with various values of p_0 and p_1, and by equations (13) and (15) for the isograin model with various values of ω_1 and ω_2. Assumed refractive index spectra in Figure 4b were used for all calculations. Q_S and Q_T of Hapke's model and s and t of the isograin model were also obtained. Those single-grain properties were linearly combined by equations (9) and (14), and the mixing ratios were optimized for the best fits between calculated and measured reflectance spectra of 16 mixtures.

Shown in Figure 8 are the root mean square deviations (RMSD) of calculated mixing ratios and reflectances for various possible combinations of ω_1 and ω_2, and p_0 and p_1. A region around the point $\omega_1 = \omega_2 = 0.3$ gives the best reproduction of mixing ratios and reflectance spectra for the isograin model, and p_0=0.5 and p_1=0.6 for Hapke's model. Those ω_1 and ω_2 values are close to 0.33 obtained for glasses in *Hiroi and Pieters* [1992]. The above values of ω_1, ω_2, p_0, and p_1 are used throughout the following calculations.

The measured and calculated reflectance spectra are shown in Figure 9, and their RMSD values are listed in Table 2. The actual and optimized mixing ratios are also listed in Table 2 and plotted in Figure 10. Both models could estimate the mixing ratios within 2.6 wt% errors.

Effective Grain Sizes for Mixtures of Grain Size <25 μm

Because the smallest grain size fractions (<25 μm) can have very different grain size distributions from one mineral to another, the effective grain sizes must be used to produce the appropriate total scattering cross sections in equations (9) and (14) for a better estimation of the mixing ratios of their mixtures.

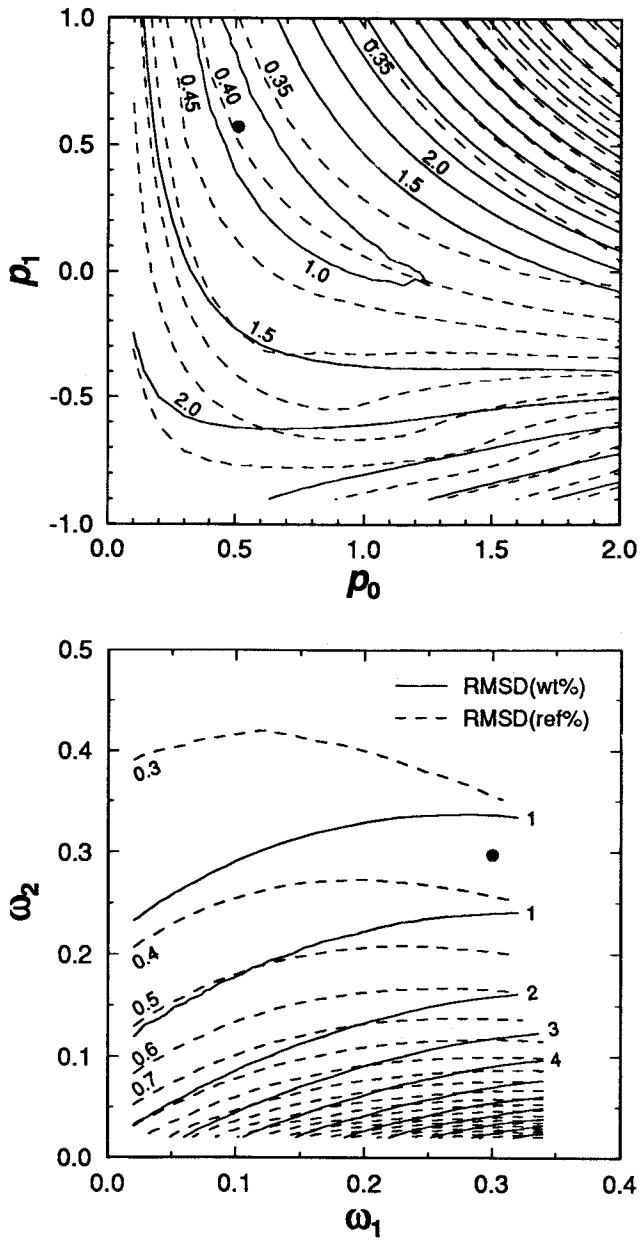

Figure 8. Contour maps of the Root Mean Square Deviation (RMSD) of calculated mixing ratios and reflectances of tricomponent mixtures (45-75 μm) for the possible values of p_0 and p_1 of Hapke's model, and ω_1 and ω_2 of the isograin model. Solid contours are for the mixing wt%, and the dashed contours are for reflectances. Solid circles indicate the chosen values ($p_0 = 0.5$, $p_1 = 0.6$, $\omega_1 = \omega_2 = 0.3$).

Reflectance spectra of seven tricomponent mixtures of grain size <25 μm in Figure 2b were fit with their end-member spectra shown in Figure 1. The obtained relative scattering cross sections σ_i of component minerals in equations (9a) and (14) were converted into the mass fractions M_i by equation (9b) for various values of the effective grain size d_e, and the RMSD of the obtained mixing ratios (wt%) were calculated.

The RMSD values for various d_e combinations are shown in Figure 11. Because only the relative effective grain sizes are important for mixing, the effective grain sizes relative to the one for olivine are used in Figure 11. Both Hapke's model and the isograin model give the best estimation of the mixing ratio with the effective grain sizes of pyroxene significantly smaller than the others. The best effective grain size ratios are Px/Ol = 0.740 and Pl/Ol = 0.939 for Hapke's model, and Px/Ol = 0.722 and Pl/Ol = 0.991 for the isograin model. The calculated and measured reflectance spectra of the mixtures are compared in Figure 12, and the mixing ratios estimated with the above effective grain size ratios are compared with the actual ones in Figure 13. The results are also summarized in Table 3. Both models could estimate the mixing ratios within 4.1 wt% errors.

End-Member Reflectance Spectra of Smaller Grain Sizes

Based on the good results of two reflectance models for mineral mixtures of grain size 45-75 μm, powders of smaller grain sizes are studied here. Shown in Figure 14 are the best spectral fits of the end-member minerals of grain sizes <25 and 25-45 μm calculated from the absorption coefficients derived for 45-75 μm by optimizing the effective grain sizes (d_e) in equations (12c) and (15c). It is clear that calculated reflectance spectra of the <25 μm fractions have absorption bands which are too deep compared to the measured spectra. The optimized effective grain sizes for the finer powders summarized in Table 4 appear unreasonably large.

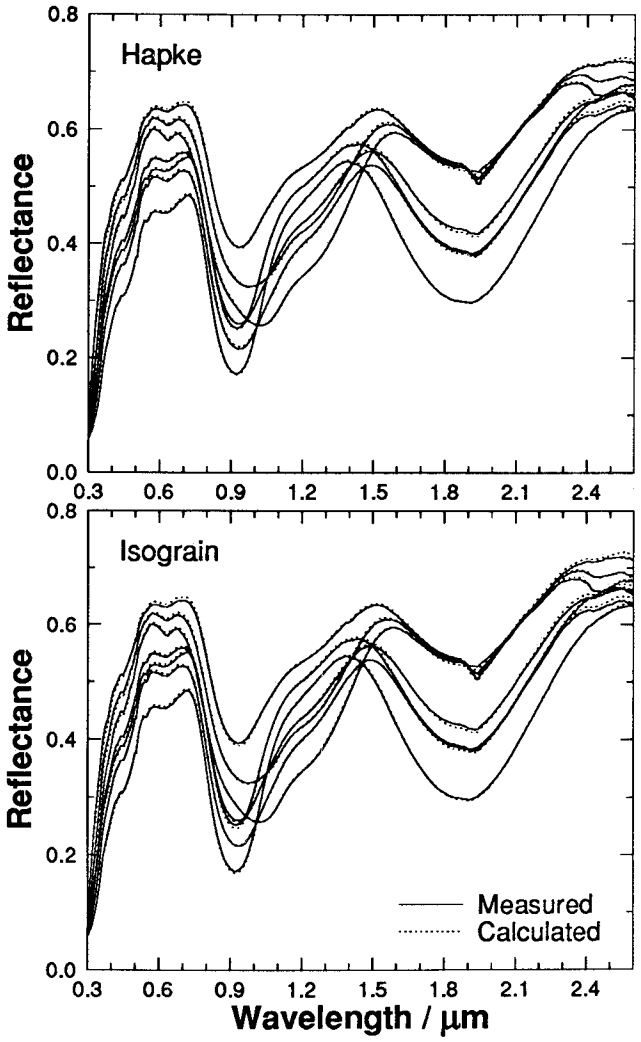

Figure 9. Model fits of reflectance spectra of tricomponent mixtures (45-75 μm) by Hapke's model ($p_0 = 0.5$, $p_1 = 0.6$) and the isograin model ($\omega_1 = \omega_2 = 0.3$).

Table 2. Actual and Calculated Mixing Ratios (wt%) of Olivine (Ol), Pyroxene (Px), and Plagioclase (Pl) and the Root Mean Square Deviations (RMSD %) of Reflectance Spectra of Tricomponent Mixtures (45-75 μm) by Hapke's Model (p_0=0.5, p_1=0.6) and the Isograin Model ($\omega_1 = \omega_2 = 0.3$)

Actual wt%			Hapke				Isograin			
Ol	Px	Pl	Ol	Px	Pl	RMSD	Ol	Px	Pl	RMSD
75.00	0.00	25.00	75.48	0.00	24.52	0.474	75.04	0.00	24.96	0.360
50.00	0.00	50.00	48.19	0.00	51.81	0.779	48.32	0.00	51.68	0.647
25.00	0.00	75.00	23.59	0.00	76.41	0.677	23.96	0.00	76.04	0.628
0.00	25.00	75.00	0.16	24.72	75.12	0.372	0.11	25.02	74.87	0.466
0.00	50.00	50.00	0.03	51.89	48.08	0.353	0.01	52.04	47.95	0.410
0.00	75.00	25.00	0.61	76.91	22.48	0.178	0.62	76.94	22.44	0.206
25.00	75.00	0.00	23.61	76.26	0.13	0.259	23.55	76.43	0.01	0.282
50.00	50.00	0.00	48.19	50.67	1.14	0.320	47.73	51.12	1.15	0.363
75.00	25.00	0.00	76.90	23.76	0.35	0.336	74.73	24.44	0.83	0.230
66.67	16.67	16.67	66.81	16.44	16.75	0.279	65.84	17.00	17.15	0.368
16.67	66.67	16.67	16.01	67.54	16.45	0.190	16.02	67.68	16.30	0.231
16.67	16.67	66.67	16.32	16.39	67.30	0.330	16.31	16.71	66.99	0.425
33.33	33.33	33.33	32.72	33.81	33.47	0.334	32.49	34.19	33.32	0.405
16.67	41.67	41.67	16.25	42.15	41.59	0.345	16.24	42.40	41.36	0.423
41.67	16.67	41.67	41.40	16.35	42.26	0.309	41.01	16.77	42.22	0.369
41.67	41.67	16.67	41.80	41.40	16.81	0.248	41.44	41.82	16.74	0.230

The effective grain sizes are fixed to 60 μm.

Both the band strengths and the calculated effective grain sizes suggest that the actual effective grain sizes are much smaller than those values and the ideal reflectances are much higher than measured.

It is hypothesized that some of the apparent decrease in reflectance and absorption strength for smaller grain sizes could be due to the surface roughness effect. The formulation of the surface-roughness effect in equations (16) and (17) was applied to the three end-member spectra of grain size <25 μm. In order to best reproduce those reflectance spectra, n_h and d_e values are optimized for various m_h values. The results are shown in Figure 15. Neither d_e nor the RMSD varies significantly with m_h. On the other hand, there is a direct relation between n_h and m_h. Since there seems to be no minimum point of the RMSD values in these calculations, a value of m_h=40 was chosen to illustrate the effects of surface roughness on the accuracy of the reflectance models.

Reflectance spectra of both <25 and 25-45 μm fractions were calculated with a surface roughness correction and are shown in Figure 16. The spectral comparison and effective grain sizes are greatly improved compared with those in Figure 14, especially for the <25 μm fractions. However, given a value of m_h it was impossible to reproduce their reflectance spectra any better through the entire wavelength range of 0.3-2.6 μm at the same time for pyroxene and plagioclase.

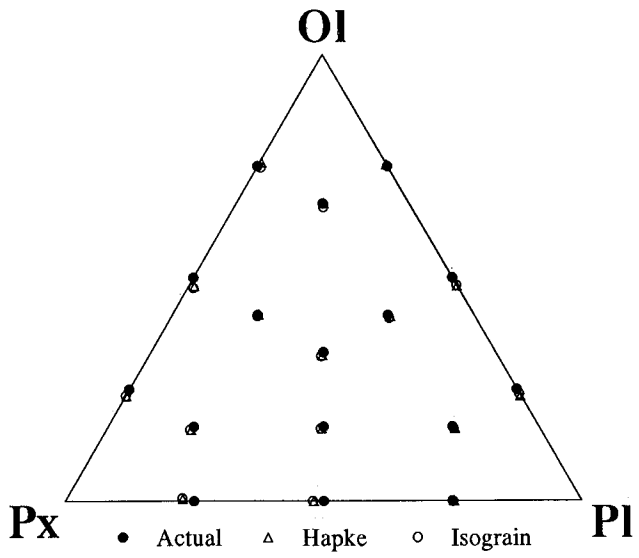

Figure 10. A plot of the actual and calculated mixing ratios (wt%) of mixtures (45-75 μm) by Hapke's model and the isograin model. All the effective grain sizes are fixed to 60 μm.

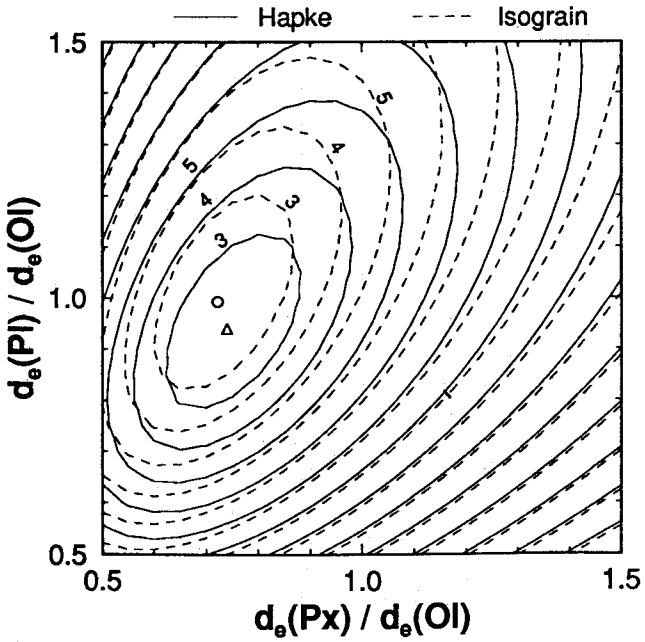

Figure 11. A contour map of the RMSD of calculated mixing ratios (wt%) of tricomponent mixtures (<25 μm) for the various effective grain size ratios. A triangle and an open circle indicate the best effective grain size ratios for Hapke's model and the isograin model, respectively.

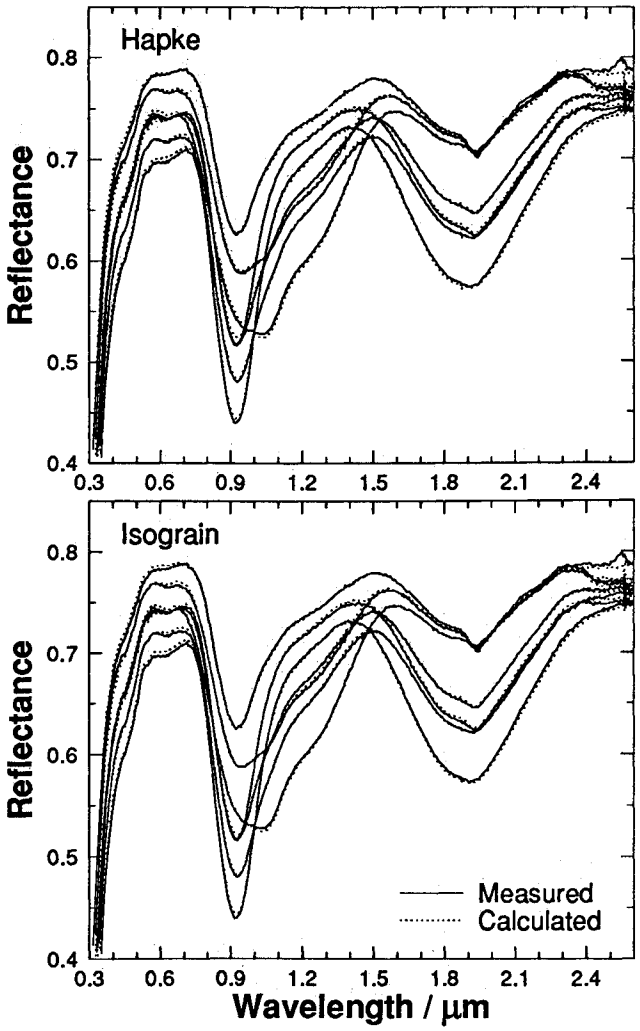

Figure 12. Model fits of reflectance spectra of tricomponent mixtures (<25 μm) by Hapke's model ($p_0 = 0.5$, $p_1 = 0.6$) and the isograin model ($\omega_1 = \omega_2 = 0.3$) using the optimized effective grain sizes (Figure 11).

All the above results are summarized in Table 4. There is significant improvement in the estimated effective grain size for all the <25 μm size fractions. There is less effect, however, for the 25-45 μm fractions. The estimated effective grain size for 25-45 μm plagioclase still appears unreasonably large with this formulation.

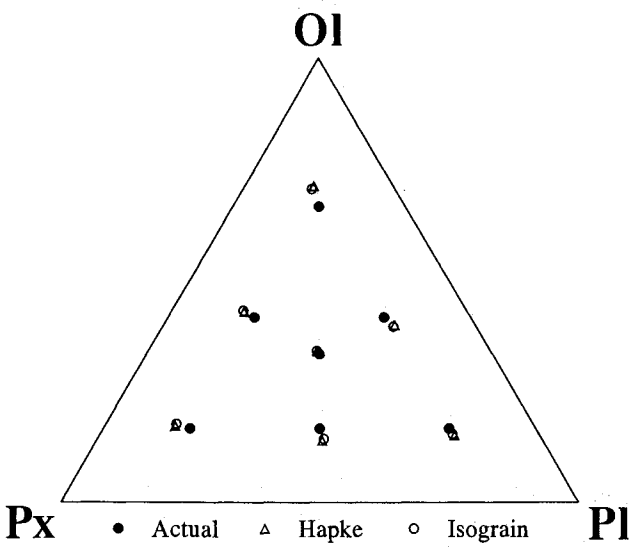

Figure 13. A plot of the actual and calculated mixing ratios (wt%) of tricomponent mixtures (<25 μm) by Hapke's model and the isograin model. The optimized effective grain size ratios in Figure 11 are used.

7. Discussion

The overall validity of two models for intimate mixtures (nonlinear mixing), Hapke's model and the isograin model, are almost identical for the mixing of the common geologic transparent minerals under the configurations in this paper. Both models employ two-stream approximation for their multiscattering part [*Hapke*, 1981; *Hiroi and Pieters*, 1992] and allow mineral abundances to be estimated. The accuracy of the multiscattering part of Hapke's model depends on its assumption of the isotropic scattering and approximation of the H function especially for large single scattering albedos, where the H function is highly nonlinear. This study has incorporated Chandrasekhar's exact solutions in Hapke's model by employing a nonlinear interpolation. Other methods of interpolation may give somewhat different results. The isograin model has no such difficulty because it exactly sums up all the transmitted and scattered light by its design. However, the viewing geometry is not incorporated in the isograin model, and Hapke's model is more appropriate in photometrical applications.

Effective grain size and surface roughness have particularly strong effects on the smallest grain sizes. If the effective grain size is optimized for the <25 μm size fraction in the mixing

Table 3. Actual and Calculated Mixing Ratios (wt%) and the RMSD (Reflectance %) of Tricomponent Mixtures (<25 μm)

Actual wt%			Hapke				Isograin			
Ol	Px	Pl	Ol	Px	Pl	RMSD	Ol	Px	Pl	RMSD
66.67	16.67	16.67	71.29	15.35	13.36	0.361	70.58	16.02	13.40	0.280
16.67	66.67	16.67	17.21	69.20	13.59	0.356	17.66	68.72	13.61	0.327
16.67	16.67	66.67	15.11	16.42	68.47	0.347	15.39	16.66	67.95	0.272
33.33	33.33	33.33	34.03	33.47	32.50	0.295	34.05	33.47	32.48	0.307
16.67	41.67	41.67	14.02	42.44	43.54	0.352	14.35	42.01	43.64	0.416
41.67	16.67	41.67	39.94	15.50	44.57	0.331	39.58	15.92	44.50	0.439
41.67	41.67	16.67	42.98	43.00	14.02	0.261	43.13	43.03	13.84	0.287

The effective grain size ratios are Px/Ol = 0.740 and Pl/Ol = 0.939 for Hapke's model, and Px/Ol = 0.722 and Pl/Ol = 0.991 for the isograin model. No surface roughness is assumed (n_h=0).

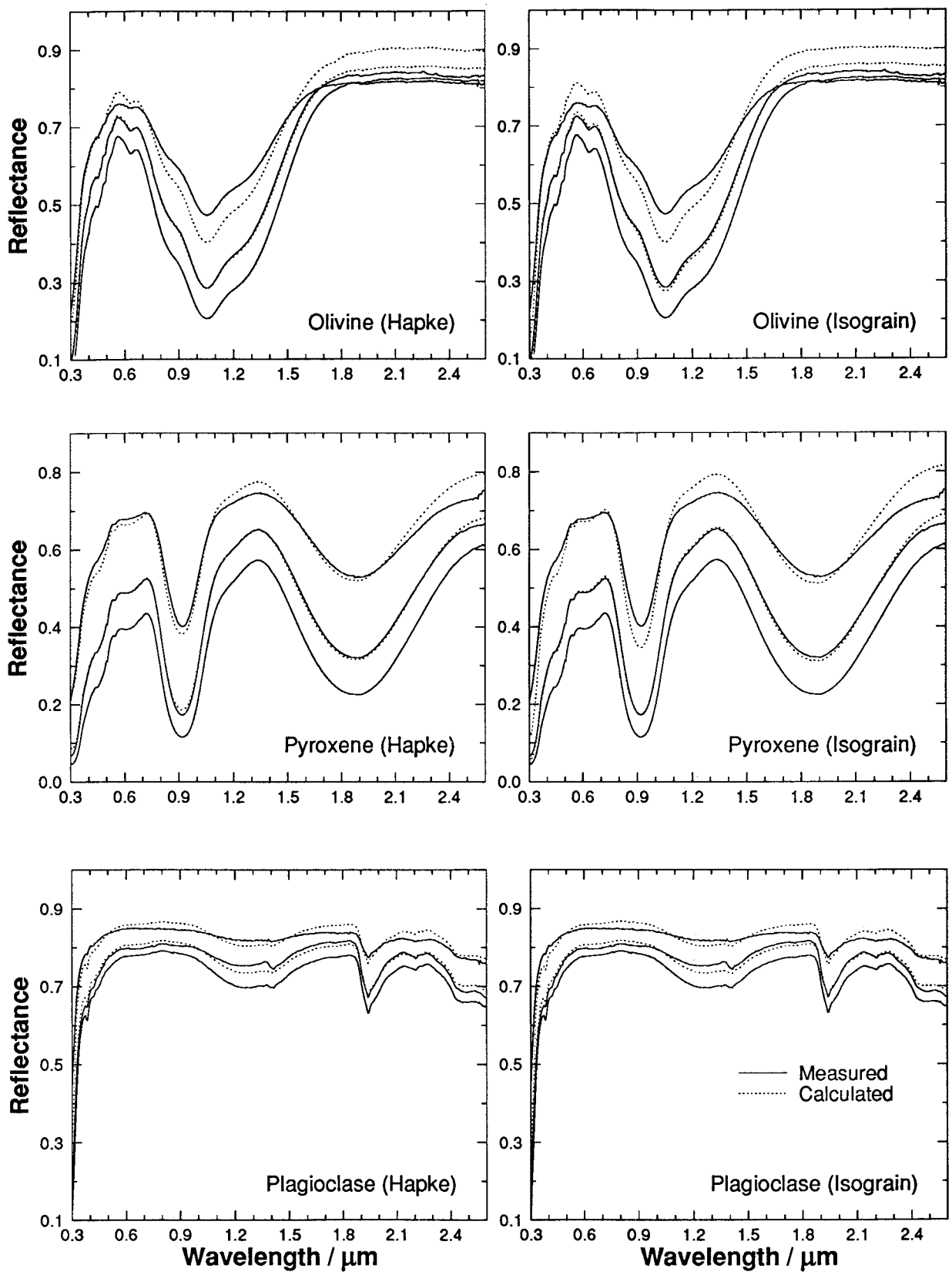

Figure 14. Model fits of reflectance spectra of three grain size fractions of three end-member minerals using the absorption coefficient derived from the 45-75 μm samples. Effective grain sizes are optimized for <25 and 25-45 μm fractions for the best fits of their reflectance spectra using the absorption coefficients derived for the 45-75 μm fraction.

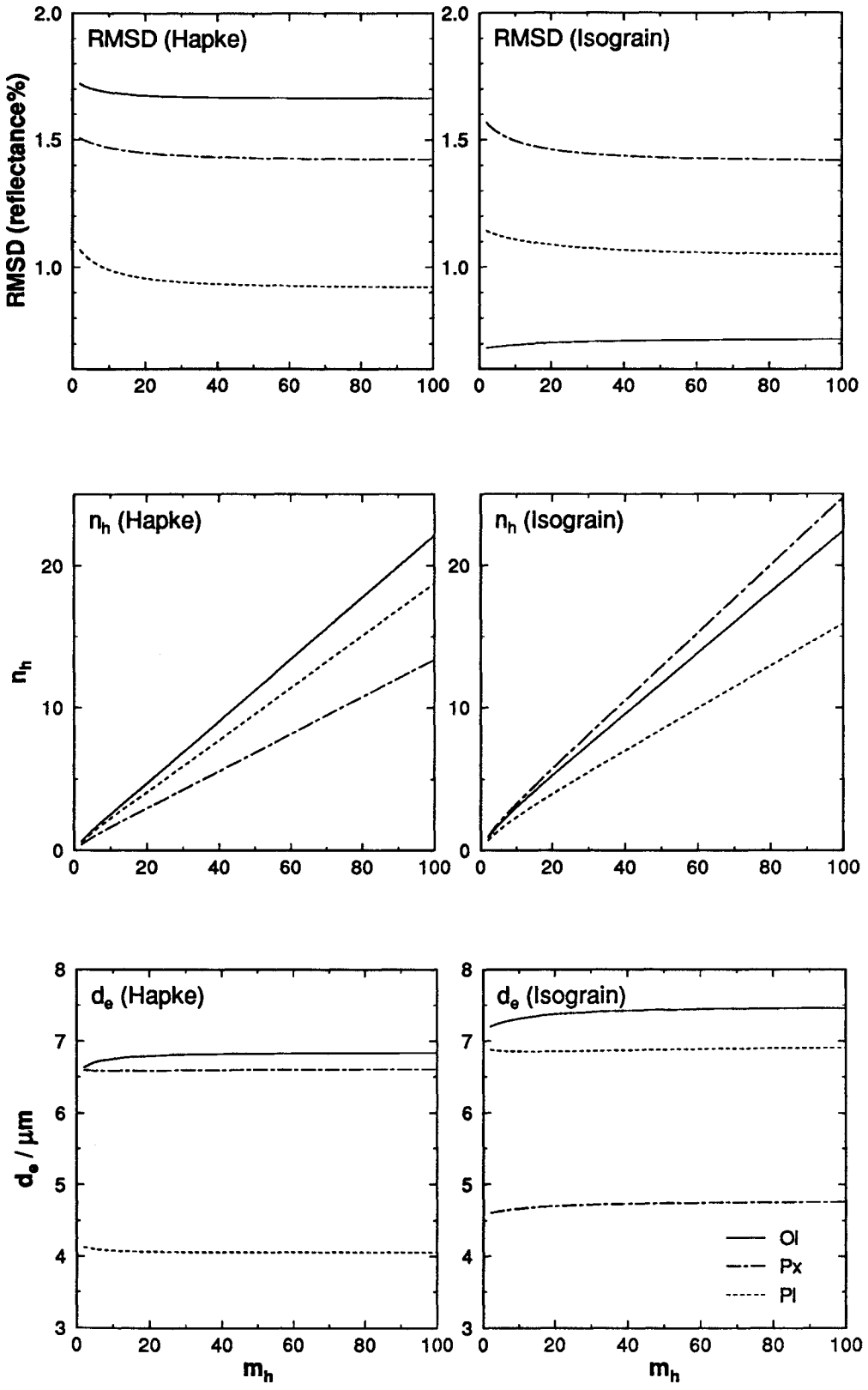

Figure 15. RMSD of reflectances, n_h, and effective grain sizes (d_e) of end-member minerals (<25 μm) for various values of m_h.

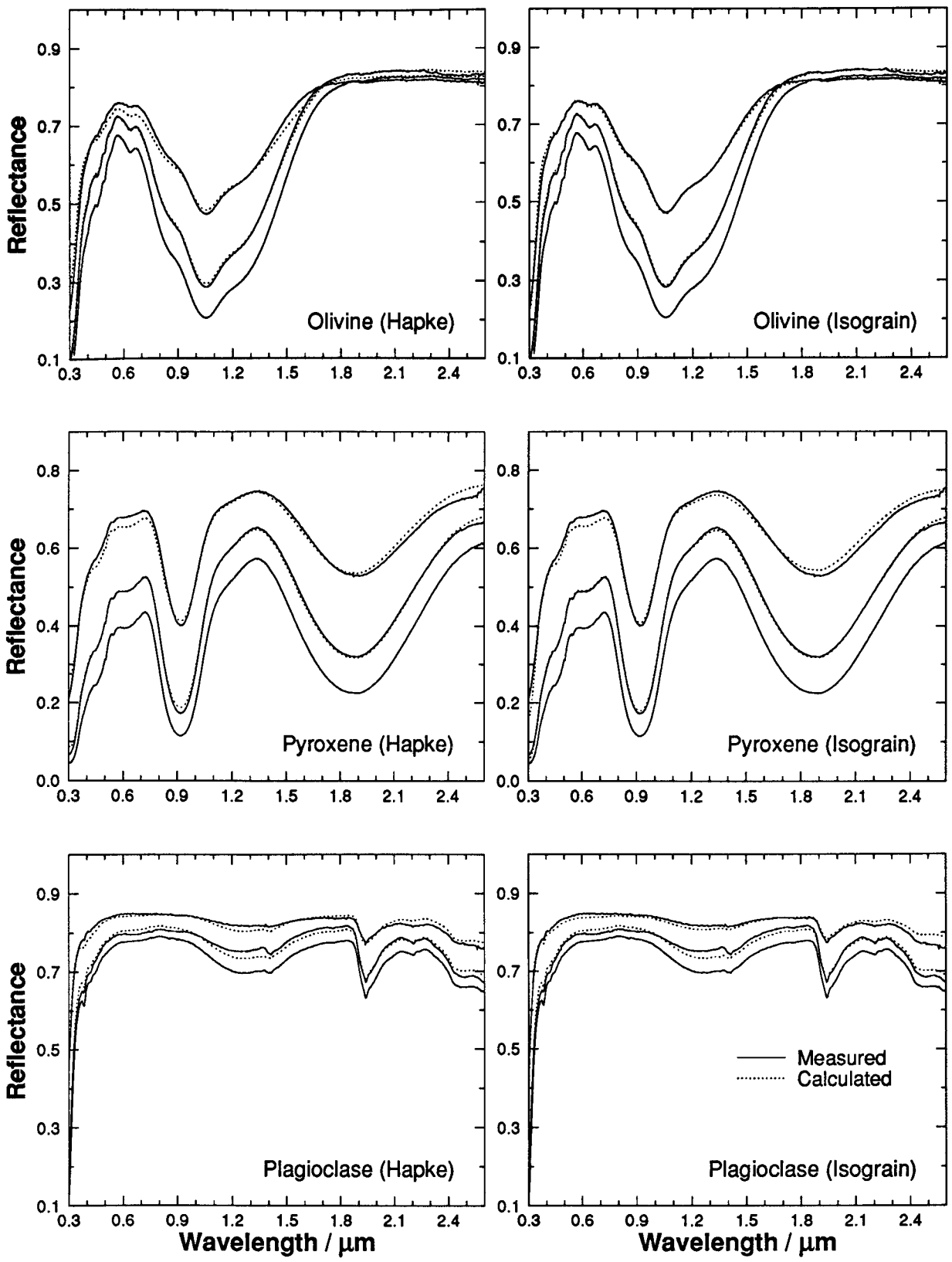

Figure 16. Same as Figure 14 with the surface-roughness correction. Parameter m_h is fixed to 40, and effective grain sizes and the n_h values are optimized individually.

Table 4. Calculated Effective Grain Sizes (d_e) and RMSD (Reflectance %) of Three Grain Size Fractions of Olivine (Ol), Pyroxene (Px), and Plagioclase (Pl)

		No Surface Roughness				With Surface Roughness (m_h=40)					
		d_e, μm		RMSD, %		d_e, μm		n_h		RMSD %	
		<25	25-45	<25	25-45	<25	25-45	<25	25-45	<25	25-45
Hapke	Ol	17.5	35.8	6.05	1.25	6.82	32.5	9.07	1.80	1.67	0.81
	Px	9.8	33.9	2.50	0.61	6.60	33.1	5.57	0.77	1.43	0.59
	Pl	17.7	41.2	1.93	1.12	4.05	41.2	7.75	0.00	0.93	1.12
Isograin	Ol	17.0	36.8	6.25	1.59	7.42	31.3	9.57	3.23	0.71	0.76
	Px	10.2	33.9	3.98	0.79	4.73	29.6	10.52	3.87	1.44	0.43
	Pl	21.8	43.6	2.32	1.11	6.87	42.3	7.01	0.64	1.07	1.11

Effective grain sizes of 45-75 μm fractions are fixed to 60 μm.

models, relatively accurate (~4 wt%) mineral mixing ratios can be determined using spectra of <25 μm mineral end-members. On the other hand, it is much more difficult for either model to accurately predict the character of the <25 μm mineral fraction using optical constants, such as those derived from large grains. Including effects of surface roughness can account for some of the disparity in band strength and reflectance frequently observed for laboratory samples. The approximate formulation of surface roughness described here can be used with either model.

Clark and Roush [1984] demonstrated that the reflectance spectrum of coarse-grained frost can be better approximated by a computational mixture of several different grain size fractions of the same optical constants. It suggests a possibility that the significant grain size range of the <25 μm powder can not be approximated sufficiently by a single average grain size adopted in this paper. However, introducing a grain size distribution cannot explain some cases where the finest grain size fraction has lower reflectances than the coarser one at some wavelengths [e.g., *Crown and Pieters*, 1987], for which the surface roughness effect is believed to play an important role.

Since fine particles occur as part of the regolith or soil of most rocky bodies in the solar system, and in some cases have been observed to dominate the optical properties [e.g., *Pieters et al.*, 1993], the effects discussed here are particularly important to consider when attempting to derive mineral abundance information from remotely acquired spectra. Due to the complexity of the natural environment and the number of variables in any intimate mixture model, however, acquiring information about mineral constituents derived from fitting reflectance spectra using mathematical models for absorption band features [e.g., *Sunshine et al.*, 1990] will be most valuable.

Acknowledgments. We thank T. Ozawa and the University Museum of the University of Tokyo for Chichi-jima bronzite (MI21383), S. F. Pratt for reflectance measurements, and B. Hapke for helpful discussions at several science meetings. We also thank R. Clark for a constructive review of the manuscript and a program, based on which our own program was written for the *H* function estimation. RELAB is a multiuser facility supported by NASA under NAGW-748. NASA support to C. M. P. (NAGW-28) is gratefully acknowledged. A part of this work was done while T. H. held a National Research Council-NASA/JSC Research Associateship. T. H. was also supported by Yamada Science Foundation, Japan.

References

Chandrasekhar, S., *Radiative Transfer*, 393 pp., Dover, Mineola, N. Y., 1960.

Clark, R. N., and T. L. Roush, Reflectance spectroscopy: Quantitative analysis techniques for remote sensing applications, *J. Geophys. Res.*, *89*, 6329-6340, 1984.

Crown, D. A., and C. M. Pieters, Spectral properties of plagioclase and pyroxene mixtures and the interpretation of lunar soil spectra, *Icarus*, *72*, 492-506, 1987.

Hapke, B., Bidirectional reflectance spectroscopy, 1, Theory, *J. Geophys. Res.*, *86*, 3039-3054, 1981.

Hiroi, T., and C. M. Pieters, Effects of grain size and shape in modeling reflectance spectra of mineral mixtures, *Proc. Lunar Planet. Sci.*, *22*, 313-325, 1992.

Hiroi, T., and H. Takeda, A method to determine silicate abundances from reflectance spectra with applications to asteroid 29 Amphitrite associating it with primitive achondrite meteorites, *Icarus*, *88*, 205-227, 1990.

Johnson, P. E., M. O. Smith, and J. B. Adams, Simple algorithms for remote determination of mineral abundances and particle sizes from reflectance spectra, *J. Geophys. Res.*, *97*, 2649-2657, 1992.

Mustard, J. F., and C. M. Pieters, Photometric phase functions of common geologic minerals and applications to quantitative analysis of mineral mixture reflectance spectra, *J. Geophys. Res.*, *94*, 13,619-13,634, 1989.

Pieters, C. M., Strength of mineral absorption features in the transmitted component of near-infrared reflected light: First results from RELAB, *J. Geophys. Res.*, *88*, 9534-9544, 1983.

Pieters, C. M., E. M. Fischer, O. Rode, and A. Basu, Optical effects of space weathering: The role of the finest fraction, *J. Geophys. Res.*, *98*, 20,817-20,824, 1993.

Sunshine, J. M., C. M. Pieters, and S. F. Pratt, Deconvolution of mineral absorption bands: An improved approach, *J. Geophys. Res.*, *95*, 6955-6966, 1990.

T. Hiroi, SN3, NASA Johnson Space Center, Houston, TX 77058. (e-mail: hiroi@sn.jsc.nasa.gov)

C. M. Pieters, Department of Geological Sciences, Brown University, Providence, RI 02912. (e-mail: cpieters@nasamail.nasa.gov)

(Received December 21, 1992: revised March 28, 1994; accepted March 28, 1994.)